Early diagenesis of radium 226 and radium 228 in lacustrine sediments influenced by former mining sites

Arnaud Mangeret[a1]. Jean-Louis Reyss[b]. Marina Seder-Colomina[a], Lucie Stetten[a, c], Guillaume Morin[c], Antoine Thouvenot[d], Marc Souhaut[e], Pieter van Beek[e]

a Institut de Radioprotection et de Sureté Nucléaire (IRSN). PSE-ENV. BP 17. Fontenay-aux-Roses. 92262 France

b Laboratoire des Sciences du Climat et de l'Environnement (LSCE/IPSL, CEA-CNRS-UVSQ, Université Paris-Saclay, ç1198 Gif-sur-Yvette, France

c Institut de Minéralogie, de Physique des Matériaux et de Cosmochimie (IMPMC), UMR 7590 CNRS-Sorbonne Université IRD-MNHN, 4 place Jussieu, 75252 Paris cedex 5, France

d Laboratoire Microorganismes Génôme et Environnement (LMGE) UMR CNRS 6023, Aubière, 63177 Aubière, France

e Laboratoire d'Études en Géophysique et en Océanographie Spatiale (LEGOS, CNRS/CNES/IRD/UPS), Observatoire Midi-Pyrénées, 14 avenue Edouard Belin, 31400 Toulouse, France

[1] Corresponding author: arnaud.mangeret@irsn.fr, Tel: +33158357695, Fax: +33146576258

Highlights

The early diagenesis of long-lived radium isotopes ^{226}Ra and ^{228}Ra was evaluated in U-mining impacted granitic lake sediments

Ra activities in sediment pore waters were measured for the first time using very low background Germanium well detectors

^{226}Ra and ^{228}Ra early diagenesis seem to be closely related to the reductive dissolution of iron oxyhydroxides

Calculated diffusive fluxes of Ra are significantly lower than those previously reported in Ra-enriched sediments

ABSTRACT

Radium is a naturally occurring radioactive element commonly found at low levels in natural systems such as lacustrine or marine sediments. Anthropogenic activities including former uranium mining activities can lead to the dissemination of radium isotopes having high radiological toxicities, which potentially threaten the safety of nearby environments. Although radium mobility in oxidized environments is known to be largely governed by sorption/desorption onto Fe and Mn oxyhydroxides and coprecipitation with sulfate minerals (e.g. barite), little is known regarding its behavior under reducing conditions, which are the conditions typically encountered in organic-rich systems such as wetlands and lake sediments. The present study aims at understanding the behavior of long-lived radium isotopes (^{226}Ra and ^{228}Ra), during early diagenesis of lake sediments contaminated by former uranium mining activities. Solid and pore water concentrations of ^{226}Ra and ^{228}Ra were determined using ultra low background gamma spectrometry, which allowed improvement of detection limits and measurement accuracy.

This study shows that the downcore distribution of radium isotopes is closely related to the reductive dissolution of iron and manganese oxyhydroxides below the sediment-water interface. The resulting diffusive fluxes of ^{226}Ra and ^{228}Ra ($4.1\ 10^{-25}$ and $4.7\ 10^{-28}$ mol.cm^{-2}.s^{-1}) are however significantly lower than other radium-impacted environments, such as uranium mill tailings pond and phosphate industry-impacted sediments, and are similar to those reported for natural marine environments. Hence, in the reduced lake sediments of Saint-Clement, the major fraction of radium is trapped by the solid phase, while early diagenesis only induces a slight mobility of this radioelement.

1. INTRODUCTION

Uranium extraction activities generate high amounts of potentially hazardous byproducts including waste rocks, mill tailings, and can also impact lands, river and lake sediments (Abdelouas, 2006, Morin et al., 2016), which can result in their enrichment in natural radionuclides such as ^{226}Ra (Carvalho et al., 2014; Reyss et al., 2016). Due to the radiotoxicity of this radionuclide, contaminated materials must therefore be appropriately managed in the long term in order to minimize its potential migration to and accumulation in human and ecological targets.

To date, the knowledge on radium mobility and dynamics in low-temperature natural systems is firstly derived from studies conducted in the marine environment. Radium isotopes are indeed frequently used as proxies for the determination of groundwater discharge fluxes into the coastal ocean (Moore, 1996; Krest and Harvey, 2003) and transport of pore water solutes (Sun and Torgensen, 2001). In these environments, the distribution of radium is known to be indirectly controlled by redox processes. For example, radium-bearing phases can be sensitive to redox variations, especially iron and manganese (oxyhydr)oxides and oxides, respectively (Gao et al., 2010; Nirdosh et al., 1984, 1990) and sulfate minerals such as barite (Doerner and Hoskins, 1925; Henkel et al., 2012).

The current knowledge of radium geochemistry in natural systems is also derived from studies conducted in continental systems (Greeman et al., 1999; Rihs et al., 2011) or in radium-enriched waste such as uranium mill tailings and adjacent surface waters and ponds (Sebesta et al., 1981; Wiles, 1983; Landa and Gray, 1995; Peacey et al., 2002; Martin et al., 2003). Although a large number of studies have addressed the radium behavior in marine and continental systems, less is known about the processes governing the fate of radium isotopes from reducing environments, except for the study of Martin et al. (2003) conducted in a tailing pond. Notably,

the influence of early diagenesis processes on the stability of radium-bearing species in reduced lake sediments is poorly documented. This knowledge is however crucial to choose the appropriate strategy to manage radium-enriched sediments.

The lack of data is notably significant regarding processes that could control radium mobility in anaerobic systems. This gap is partly related to the challenges encountered for i) sampling significant volumes of anaerobic sediment pore waters without modifying radium distribution and ii) measuring low radium isotopes activities in these pore waters. As an example, the study of Gao et al. (2010) leads to the quantification of low ^{226}Ra fluxes from sediments to the overlying waters based on the use of Diffusive Gradient in Thin Films (DGT) techniques and concludes that labile ^{226}Ra can be related to the reductive dissolution of iron and manganese (oxyhydr)oxides without clearly demonstrating the close association between Ra and Fe association in the solid phase.

The present study aims at providing relevant clues on the geochemical processes controlling the radium distribution in the sedimentary column of a lake. The behavior of ^{226}Ra is compared with analogous solutes such as ^{228}Ra and barium. The obtained results reveal important geochemical factors that may be considered for better predicting the post-depositional mobility of radium isotopes in impacted lacustrine systems, as well as, by extension, in underwater radioactive waste storage.

2. MATERIALS AND METHODS

2.1 Site description and sampling procedures for sediment and pore water

The lake Saint-Clément is an artificial reservoir created in 1931 for electricity generation. This lake is located at nearly 20 kilometers downstream from the former uranium mining site of Bois-Noirs-Limouzat and its tailing storage in the Massif Central (Figure 1).

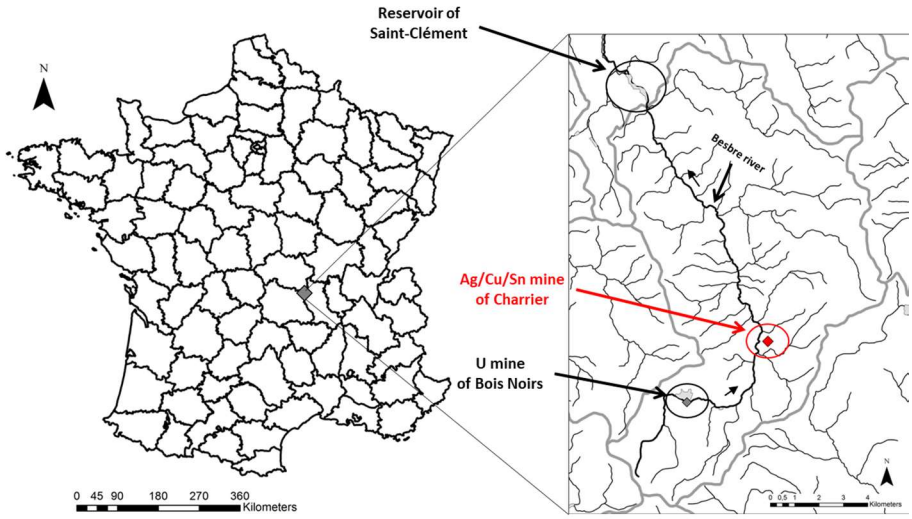


Fig. 1 *Map of the lake of Saint-Clément (Allier, France) and the core sampling station d from the French hydrographic network database CARTHAGE®). The lake of Saint-Clément is supplied by the river Besbre.*

A detailed description of the site can be found in Morin et al. (2016), Reyss et al. (2016) and Stetten et al. (2018a). Lake sediment cores were sampled within PVC liners using a 90 mm diameter Uwitec® hand corer. Sediments cores were collected at location C2 situated about 100 m upstream from the dam (Reyss et al., 2016), in October 2015 and May 2016, i.e. cores 2015C2G and 2016C2I, respectively. Immediately after sampling, the cores were placed in a glove bag previously purged three times with N_2. Volumes of 15-25 mL of pore waters were

extracted from sediments every 5 cm using 0.15 µm pore size Rhizons® samplers. Each of them was connected to a glass vial that had been previously purged with N_2 in an anaerobic glove box in the laboratory. Field and laboratory sampling and storage procedures are detailed in Stetten et al. (2018a). Solids were sampled every 5 cm along the core and dried at 30°C before analysis.

2.2 Analyses of major and minor elements in sediments and pore waters

The analyses of major and trace elements in the solid sediment samples were performed at the IRSN/LUTECE laboratory with a ICP-OES Thermo Fisher ICap 7600 Duo and an Agilent 8800 ICP-MS/MS (Agilent Technologies, Japan), after acid digestion according to the same procedures as previously described by Stetten et al. (2018a).

The measurements of pH, alkalinity and dissolved Fe(II) in pore waters were performed in an anoxic glove-box (< 5 ppm O_2) at the IMPMC laboratory within 48 hours after sampling. Alkalinity measurements were performed following the procedure described previously by Sarazin et al. (1999). Dissolved Fe(II) was determined by a colorimetric method adapted from the classical orthophenanthroline method (Fadrus and Malỳ, 1975). A detailed description of the two latter analyses can be found in Stetten et al. (2018a).Uranium and trace metals analyses in pore waters were performed at the IRSN/LUTECE laboratory with ICP-MS Thermo Fisher X7 Serie 1. Major and trace elements analyses were performed using an ICP-OES ICap 7600 Duo Thermo Fisher. Measurements were performed using external standard solutions and uncertainties were estimated from 5 replicate measurements on the standard solutions.

2.3 Quantification of radionuclides in sediments and pore waters

For sediment samples, aliquots of 1-4 g were used for measuring ^{238}U and ^{232}Th-series nuclide activities using the High Purity Germanium well-type detector of the IRSN/LUTECE laboratory (GWL-220-15). ^{210}Pb, ^{234}Th (considered in equilibrium with ^{238}U), ^{214}Pb and ^{214}Bi (^{226}Ra), ^{228}Ac (^{228}Ra), ^{212}Pb and ^{208}Tl (^{228}Th) were analyzed after a counting time of one day. The measurement procedures were similar to those reported by Reyss et al. (1995, 2016). The gamma detector was calibrated using several international IAEA standards such as RGU-1, RGTh-1, IAEA-312 and 314.

The determination of ^{226}Ra and ^{228}Ra activities in pore water samples was performed at the "Laboratoire Souterrain of Modane" in the French Alps (Cazala et al., 2003; Reyss et al., 1995). The pore water samples (15-30 mL) were thereafter evaporated until a final volume of 5 mL was reached. A counting time of 3-5 days was required to achieve a 1σ statistical error lower than 10% (Reyss et al., 1995). Activities of ^{232}Th activities in the sediment solid phase were assumed to be at an average level of 140 Bq.kg^{-1}, as previously reported in the sediments of the two sampling stations located close to the dam of the lake Saint-Clément (Reyss et al., 2016).

2.4 Selective chemical extraction procedures

Selective chemical extraction procedures were applied to the sediment to identify the different phases that carry Ra. The proportions of ^{226}Ra and ^{228}Ra in the extractable (FE), reducible (FRED) and oxidizable fractions (FOX) of the sediments were assessed. Two grams of samples representative of sparsely (10-15 cm) and mining-impacted (110-115 cm) sediments were used for each extraction condition. The boundary between the two types of sediments samples was

fixed at 92.5 cm depth, due to the simultaneous increase of solid ^{238}U, ^{226}Ra and ^{210}Pb as was previously reported (Reyss et al., 2016).

First, the sediment was placed with 40 mL of 1M $Mg(NO_3)_2$ stirred during 2 h at ambient temperature and then washed with deionized water. This leaching procedure is expected to extract ionically and loosely bound radium, i.e. exchangeable (FE fraction). Second, radium sorbed to or coprecipitated with Fe and Mn, nano-crystalline and crystalline (oxyhydr)oxides (FRED fraction) was extracted using the Citrate-Dithionite-Bicarbonate procedure (Mehra and Jackson, 2013). Third, radium associated with organic matter (FOX fraction) was separated by oxidation with H_2O_2 under nitric media (Aguado et al., 2004). Details regarding the protocols for extracting these above-mentioned exchangeable (FE), reducible (FRED), and oxidizable (FOX) fractions can be found in Table 1.

Tab. 1: *Detailed protocols of selective chemical extraction of radium in sediments*

Reagent	Solid/Liquid Ratio	Experimental conditions	Radium fraction extracted
1M $Mg(NO_3)_2$	1: 20	2h at ambient temperature	Loosely and ionically bound Ra
0.27M $C_6H_5Na_3O_7$, $2H_2O$ 0.1M $NaHCO_3$ 2 g $Na_2S_2O_4$	2 : 75	40 min at 80°C	Ra sorbed and coprecipitated with amorphous/poorly ordered and well crystallised iron oxides
0.02M HNO_3 (1) + 30% H_2O_2; further 30% H_2O_2 (2)	1: 20	1 => 2 h at 85°C 2=> 3 h at 85°C	Radium associated with organic matter

After each type of selective extraction, the mixtures were centrifuged at 10,000 rpm and the residue was washed once with the reagent solution. All supernatant solutions were then acidified with 2% HNO_3 prior being analysed by gamma spectrometry as described previously. The Ra activities determined following each sequential leaching were then compared to the Ra activities measured in the bulk fraction.

3. RESULTS AND DISCUSSION

3.1 Vertical evolution of U and Th-series nuclides activities

Solid phase Ra concentration profiles. The activities of the ^{238}U-serie nuclides in the sediment solid phase are reported in Figure 2 and Table 2 for core 2016C2I and are roughly similar to those measured in a previous study on the same lake (Reyss et al., 2016). The activities of ^{238}U, ^{226}Ra and ^{210}Pb are fairly constant until approximately 90 cm depth, reflecting the deposition of the same sediment type until this depth. From 90 to 120 cm depth, the ^{238}U, ^{226}Ra and ^{210}Pb activities increase sharply up to 3862, 1154 and 1245 Bq.kg^{-1}, respectively. These increases in ^{238}U-series nuclide activities at depth have been previously interpreted as the legacy of former uranium mining activities that ceased at the beginning of the 1980's (Reyss et al., 2016; Stetten et al., 2018a). In addition, activities of the ^{232}Th-series have been formerly characterized in the sediments of the lake Saint-Clément, with an average value of 140 Bq.kg^{-1} for ^{232}Th activities in the solid phase (Reyss et al., 2016). Figure 1 also displays the profile of ^{228}Ra activity that is characterized by a continuous decrease with depth, from 260 to 140 Bq.kg^{-1}. Due to little variation of ^{232}Th activities, it gave an excess of ^{228}Ra, which was previously identified in the sediments of the lake Saint-Clément. This excess ^{228}Ra decrease with depth and this trend was previously interpreted as a radioactive decay and used for dating these sediment deposits (Reyss et al., 2016). According to this method, the sedimentation rate for core 2016C2I analysed in the present study is estimated at 5.2 cm.y^{-1}; which is exactly the same value obtained previously by Reyss et al. (2016) on another core that was taken in the close vicinity of our sampling station in the lake.

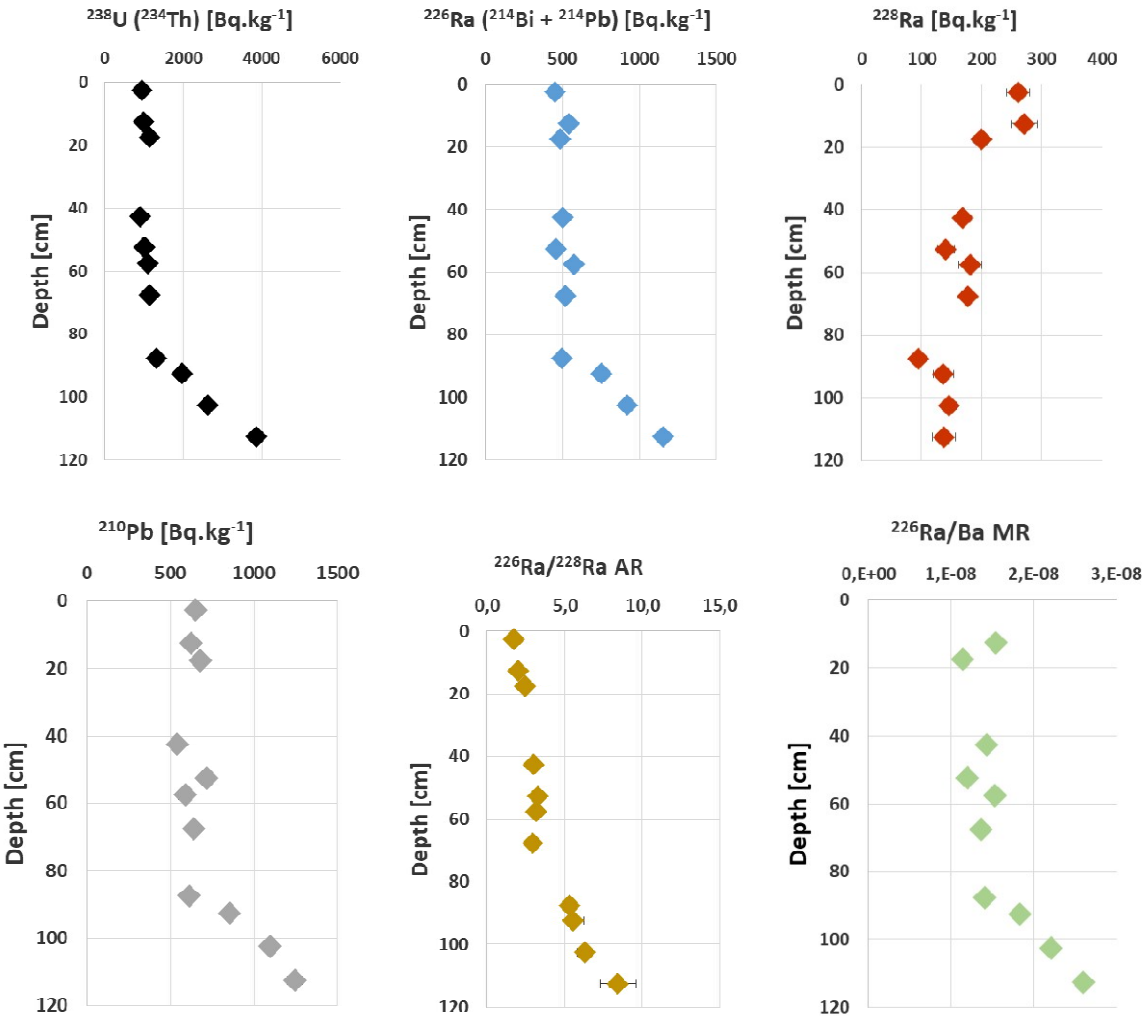


***Fig. 2**: ^{238}U and ^{232}Th-serie nuclide profiles in solid sediment samples (Bq.kg^{-1}). $^{226}Ra/^{228}Ra$ Activity Ratios (AR) are also reported together with Molar Ratio (MR) of $^{226}Ra/Ba$.*

***Tab. 2:** Activities of ^{238}U and ^{232}Th decay series nuclides in Bq per kg of dry sediments*

Sample	^{238}U (^{234}Th)	^{230}Th	^{226}Ra (^{214}Pb + ^{214}Bi)	^{210}Pb	^{228}Ra (^{228}Ac)	^{137}Cs
2.5	929 ± 39	773 ± 238	451 ± 8	649 ± 35	260 ± 19	22 ± 3
12.5	986 ± 44	712 ± 281	543 ± 10	626 ± 40	271 ± 21	21 ± 3
17.5	1126 ± 32	343 ± 204	487 ± 7	679 ± 29	200 ± 12	29 ± 2
42.5	903 ± 21	602 ± 130	502 ± 5	540 ± 18	168 ± 9	22 ± 1
52.5	996 ± 36	735 ± 215	461 ± 8	718 ± 30	140 ± 14	18 ± 2
57.5	1090 ± 45	499 ± 274	573 ± 10	589 ± 38	181 ± 19	26 ± 3
67.5	1131 ± 25	705 ± 143	521 ± 5	640 ± 21	176 ± 10	30 ± 2
87.5	1307 ± 23	240 ± 127	498 ± 5	613 ± 19	94 ± 8	24 ± 1
92.5	1957 ± 48	625 ± 257	752 ± 10	856 ± 37	136 ± 17	35 ± 3
102.5	2620 ± 37	1145 ± 189	920 ± 7	1101 ± 28	146 ± 12	52 ± 2
112.5	3862 ± 62	1043 ± 309	1154 ± 7	1245 ± 47	137 ± 19	56 ± 3

Pore water Ra concentration profiles. In the two sediment cores 2015C2G and 2016C2I, the activities of ^{226}Ra and ^{228}Ra in pore waters increase with depth, respectively ranging from 0.3 to 9.8.10^{-8} and from 0.1 to 0.7.10^{-10} µM (Figure 3, Table 3). These activities are higher than in the overlying waters of the lake, where ^{226}Ra and ^{228}Ra activities range from 1.4 to 2.3.10^{-9} and 1.4 to 2.1.10^{-12} µM respectively at 1 and 10 meters depth below the lake surface.

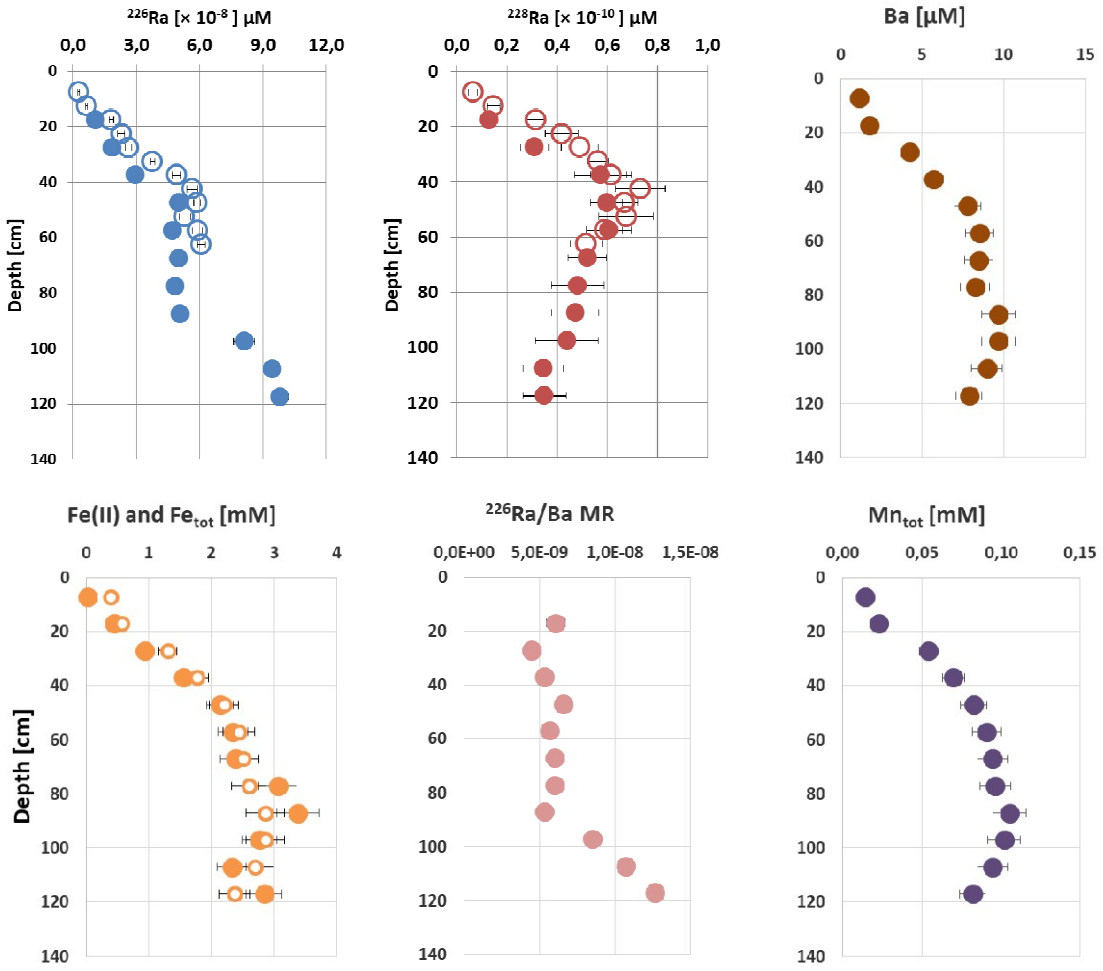


Fig. 3: *^{226}Ra, ^{228}Ra, Fe, Mn and Ba distributions in pore waters. Solid and empty red and blue circles refer respectively to 2015C2G and 2016C2I data while filled and unfilled orange circles represent total Fe and Fe(II) respectively. Molar Ratio (MR) of ^{226}Ra/Ba is also reported.*

Tab. 3: *Activities of Ra and concentrations of Fe, Mn and Ba in pore waters for the 2016C2I sediment core*

Sample	^{226}Ra (^{214}Pb + ^{214}Bi) [× 10^{-8}] µM	^{228}Ra (^{228}Ac) [× 10^{-10}] µM	Fe(II)	Fe_T mM	Mn_T	Ba_T µM
-10	0.227 ± 0.004	0.021 ± 0.001	-	-	-	-
7	-	-	0.020 ± 0.002	0.39 ± 0.04	0.014 ± 0.001	1.11 ± 0.01
17.5	1.064 ± 0.108	0.129 ± 0.026	0.44 ± 0.04	0.56 ± 0.06	0.023 ± 0.002	1.78 ± 0.18
27.5	1.866 ± 0.144	0.310 ± 0.056	0.93 ± 0.09	1.31 ± 0.14	0.054 ± 0.005	4.22 ± 0.44
37.5	2.966 ± 0.191	0.572 ± 0.103	1.55 ± 0.15	1.77 ± 0.18	0.070 ± 0.007	5.68 ± 0.58
47.5	5.023 ± 0.179	0.598 ± 0.064	2.14 ± 0.21	2.20 ± 0.23	0.083 ± 0.008	7.79 ± 0.80
57.5	4.724 ± 0.239	0.606 ± 0.090	2.34 ± 0.23	2.44 ± 0.25	0.091 ± 0.009	8.52 ± 0.87
67.5	4.999 ± 0.227	0.520 ± 0.077	2.38 ± 0.23	2.51 ± 0.25	0.095 ± 0.009	8.45 ± 0.87
77.5	4.843 ± 0.287	0.482 ± 0.103	3.06 ± 0.31	2.60 ± 0.27	0.096 ± 0.010	8.23 ± 0.87
87.5	5.094 ± 0.239	0.473 ± 0.095	3.38 ± 0.34	2.86 ± 0.30	0.106 ± 0.011	9.69 ± 1.02
97.5	8.120 ± 0.490	0.439 ± 0.125	2.77 ± 0.28	2.86 ± 0.30	0.102 ± 0.01	9.69 ± 1.02
107.5	9.459 ± 0.323	0.344 ± 0.082	2.33 ± 0.23	2.70 ± 0.29	0.095 ± 0.009	8.96 ± 0.95
117.5	9.818 ± 0.419	0.348 ± 0.086	2.85 ± 0.28	2.36 ± 0.25	0.082 ± 0.008	7.86 ± 0.80

Tab. 4 *Activities of Ra and concentrations of Fe, Mn and Ba in pore waters for the 2015C2G sediment core*

Sample	^{226}Ra (^{214}Pb + ^{214}Bi) [× 10^{-8}] µM	^{228}Ra (^{228}Ac) [× 10^{-10}] µM	Fe(II)	Fe_T mM	Mn_T	Ba_T µM
7.5	0.287 ± 0.048	0.064 ± 0.017	0.03 ± 0.00	0.13 ± 0.01	0.010 ± 0.001	0.7 ± 0.1
12.5	0.646 ± 0.048	0.146 ± 0.026	0.24 ± 0.02	0.38 ± 0.04	0.017 ± 0.002	1.0 ± 0.1
17.5	1.818 ± 0.108	0.314 ± 0.034	0.37 ± 0.04	0.51 ± 0.05	0.021 ± 0.002	1.4 ± 0.1
22.5	2.284 ± 0.167	0.417 ± 0.064	1.02 ± 0.10	-	0.052 ± 0.005	3.7 ± 0.4
27.5	2.631 ± 0.144	0,490 ± 0.073	1.51 ± 0.15	1.75 ± 0.18	0.070 ± 0.007	5.2 ± 0.5
32.5	3.767 ± 0.108	0.563 ± 0.043	1.81 ± 0.18	2.06 ± 0.21	0.080 ± 0.008	6.3 ± 0.6
37.5	4.903 ± 0.203	0.615 ± 0.082	2.12 ± 0.21	2.24 ± 0.22	0.082 ± 0.008	6.7 ± 0.7
42.5	5.645 ± 0.263	0.731 ± 0.099	2.25 ± 0.22	2.52 ± 0.25	0.090 ± 0.009	7.4 ± 0.7
47.5	5.884 ± 0.167	0.666 ± 0.056	2.29 ± 0.23	2.51 ± 0.25	0.095 ± 0.009	8.8 ± 0.9
52.5	5.286 ± 0.263	0.675 ± 0.107	2.53 ± 0.25	2.60 ± 0.26	0.098 ± 0.009	9.1 ± 0.9
57.5	5.896 ± 0.227	0.589 ± 0.073	2.43 ± 0.24	2.76 ± 0.28	0.095 ± 0.009	8.4 ± 0.8
62.5	6.063 ± 0.179	0.516 ± 0.064	2.35 ± 0.23	2.70 ± 0.27	0.098 ± 0.010	8.3 ± 0.8
67.5	6.458 ± 0.179	0.568 ± 0.064	2.56 ± 0.26	2.85 ± 0.28	0.100 ± 0.010	8.7 ± 0.9
72.5	6.888 ± 0.957	0.546 ± 0.344	2.72 ± 0.27	2.92 ± 0.29	0.104 ± 0.010	9.3 ± 0.9

Deeper in the sediment, i.e. below 40 cm, the behavior of ^{226}Ra in sediment pore waters differs from that of ^{228}Ra (Figure 3). The decrease of pore water ^{228}Ra activities with increasing depth below 40cm, can be related to its progressive radioactive decay, with its shorter half-life (5,75 years) compared to ^{226}Ra (1600 years). In contrast, dissolved ^{226}Ra activity roughly increases to 5-6.10^{-8} µM and remains constant from 40 to 90 cm depth and then increases again below 90 cm, up to 9.10^{-8} µM (Figure 3).

3.2 Radium distribution between mineral and organic phases in the sediment

In order to identify the mechanisms controlling the release of ^{226}Ra and ^{228}Ra from sediment to pore water, selective chemical extraction experiments were performed to assess the solid-state speciation of radium in the sediment core. For this purpose, a recent sediment sample and a mining-impacted one were chosen at 30 and 115 cm depth in core 2016C2I; these samples exhibited contrasting ^{226}Ra activities of 850 and 2100 Bq.kg^{-1} respectively.

Selective chemical extractions (Table 1) performed on these representative samples indicate that for the surface sediments, the exchangeable fraction contains 6.1 and 10% of total ^{226}Ra and ^{228}Ra respectively while the reducible and oxidizable fractions contain 0.7-1.3 % and 0.3-3.7% of total Ra, respectively (Figure 4). For the deep sediments, the exchangeable and oxidizable fractions display few measurable differences compared to the surface sediment samples. The reducible fraction was 6.7 and 10.3% of ^{226}Ra and ^{228}Ra, which is slightly higher than for the surface sediments. In soils and sediments, the retention of radium in the solid phase is generally reported to be controlled by adsorption onto ferric (oxyhydr)oxides and some clay minerals, as well as by coprecipitation of mineral sulfates such as barite and strontianite (Chen and Kocar, 2018). According to our chemical extractions results, the fraction of Ra associated

with Fe and Mn (oxyhydr)oxides or sorbed to clay minerals or organic matter does not exceed 7% of total Ra in the sediment.

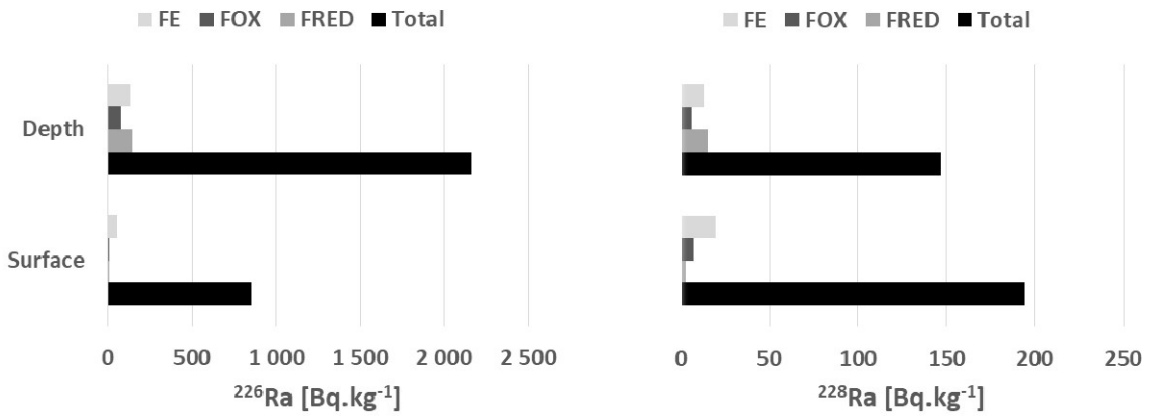


Fig. 4*: Amount of ^{226}Ra and ^{228}Ra extracted from two different sediment samples: exchangeable (FE), oxidizable (FOX) and reducible fraction (FRED). Total ^{226}Ra and ^{228}Ra in the pristine samples are also plotted for comparison.*

The residual fraction accounts for at least 93% of the ^{226}Ra and ^{228}Ra in the sediments. Previous X-ray diffraction data from Morin et al. (2016) and Stetten et al. (2018a) indicated that the mineralogical composition of the sediments of the lake Saint-Clément mainly consists of quartz, feldspar, micas and chlorite. In addition, scarce accessory minerals such as barite, pyrite and rare U-bearing minerals including zircon, thorite, monazite and rhabdophane were detected by scanning electron microscopy coupled to energy dispersive X-ray spectroscopy (SEM-EDXS) (Morin et al. 2016 ; Stetten et al. 2017). These U-bearing crystalline mineral species are expected to be resistant to our selective chemical extraction procedures and are likely the major hosts for ^{238}U and ^{232}Th decay daughters such as radium in the sediments. It is difficult to further constrain the relationship between Ra and a given mineral species because Ra concentration in the studied sediments ($1.3.10^{-5}$ mg.kg^{-1}) is far below the detection threshold for current solid-state spectroscopic techniques. Nevertheless, the mean ^{226}Ra activity in the sediments of the

lake Saint-Clément (500 $Bq.kg^{-1}$) within the first 80 cm, falls into the range of values frequently encountered in natural granitic settings (IAEA, 2014), which is consistent with a dominant occurrence of Ra in accessory minerals such as zircon, thorite, monazite and rhabdophane.

Due to similar chemical properties of the Ra^{2+} and Ba^{2+} ions, the $^{226}Ra/Ba$ ratio can be proposed as a potential proxy for the mineralogical association between these two elements. Unlike radium isotopes, the distribution of Ba content in sediment exhibits a nearly constant trend for the core studied (Table 2, Figure 5). Accordingly, the vertical evolution of the $^{226}Ra/Ba$ ratios in the solid phase of the sedimentary column clearly displays two different patterns, suggesting that i) ^{226}Ra and Ba may be carried by the same phase down to 87.5 cm depth (nearly constant $^{226}Ra/Ba$ ratios) and ii) between 87.5 and 120 cm, another ^{226}Ra-bearing phase that is likely related to former U mining inputs occurs (increasing $^{226}Ra/Ba$ ratios, Figure 5).

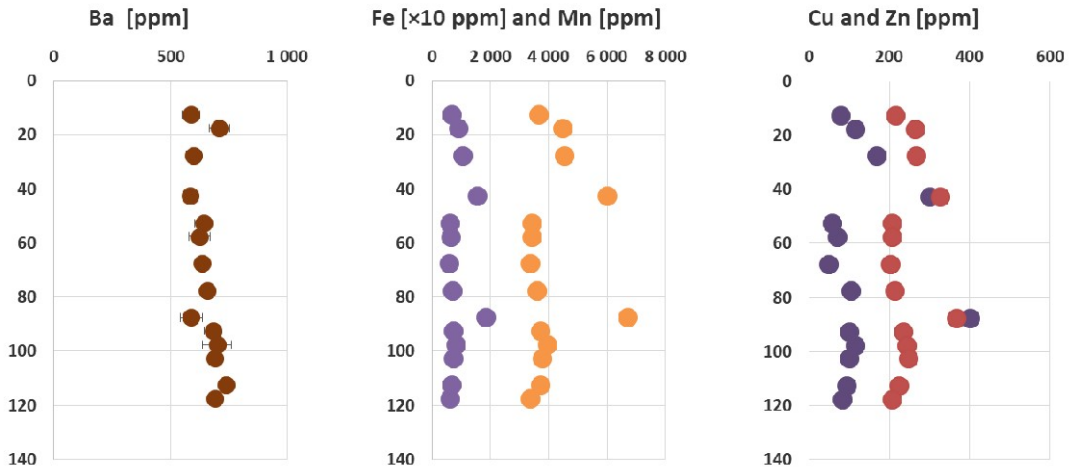


Fig. 5*: Fe, Mn, Ba, Cu and Zn concentrations associated in dry sediment samples of the lake Saint-Clément. Purple and light orange circles refer to total Fe and Mn concentrations respectively. Total Cu and Zn are respectively defined with black and red circles.*

Tab. 5: *Concentrations of metals in the solid sediment phase (expressed in mg.kg^{-1})*

Sample	Fe (%)	Mn	Cu	Ba	Zn	^{226}Ra/Ba
12.5	3.6 ± 0.4	672 ± 68	79 ± 8	588 ± 59	214 ± 7	0.9
17.5	4.5 ± 0.5	884 ± 89	114 ± 12	709 ± 71	263 ± 8	0.7
27.5	4.5 ± 0.5	1055 ± 106	168 ± 17	599 ± 60	267 ± 7	-
42.5	6.0 ± 0.6	1547 ± 155	300 ± 30	582 ± 58	325 ± 8	0.9
52.5	3.4 ± 0.4	609 ± 61	56 ± 6	641 ± 64	206 ± 7	0.7
57.5	3.4 ± 0.4	639 ± 64	70 ± 1	624 ± 63	207 ± 7	0.9
67.5	3.4 ± 0.4	573 ± 58	48 ± 5	636 ± 64	201 ± 7	0.8
77.5	3.6 ± 0.4	690 ± 69	104 ± 11	656 ± 66	213 ± 7	-
87.5	6.7 ± 0.7	1844 ± 184	402 ± 4	589 ± 59	366 ± 8	0.8
92.5	3.7 ± 0.4	710 ± 71	100 ± 10	682 ± 68	234 ± 7	1.1
97.5	4.0 ± 0.4	800 ± 80	114 ± 12	700 ± 70	243 ± 7	-
102.5	3.8 ± 0.4	736 ± 74	99 ± 9	692 ± 69	247± 8	1.3
112.5	3.70 ± 0.37	667 ± 67	93 ± 10	737 ± 74	223 ± 7	1.6
117.5	3.40 ± 0.34	613 ± 62	83 ± 8	692 ± 69	206 ± 7	-

3.3 Influence of early diagenesis on Ra mobility

Previous measurements of dissolved oxygen at the SWI in the lake Saint-Clément provide evidence of the swift development of anoxic conditions below 1-3 millimeters depth (Stetten et al., 2018a). Redox proxies such as dissolved nitrate and sulfide were previously measured in sediment pore waters and were found to be below the detection limits (Stetten et al., 2018a). Moreover, pyrite crystals were rare and of submicron size in the entire sedimentary column. These observations suggest that nitrate and sulfate reduction processes are minor in the sedimentary column.

The vertical profiles of dissolved Fe and Mn in pore waters (Figure 3) are characteristic of the reductive dissolution of iron and manganese (oxyhydr)oxides (Froelich et al., 1979). The occurrence of ferrihydrite in the sediments of the lake Saint-Clément was suggested by the measurement of 8-14% of ascorbate extractable iron in a sediment core collected at the same sampling station, in the previous study by Stetten et al. (2018a). In the same study, XANES and EXAFS analyses at the Fe K-edge indicated that Fe(III) was reduced to > 95% as Fe(II) in the solid phase below 40 cm depth, with iron being dominantly hosted in the structure of clay minerals. Minute iron (oxyhydr)oxide grains were however observed by SEM-EDXS in the 59

– 62 cm depth sample (Figure 6), in the 2012-core studied by Morin et al. (2016). Iron was found to be entirely in the form of aqueous Fe(II) in the pore waters (Stetten et al., 2018a). Dissolved barium in sediment pore waters follows the same trend as dissolved Fe and Mn ; with a maximum concentration of 10 µM at 90 cm depth. The close correlation between dissolved Fe, Mn and Ba profiles support a possible occurrence of adsorbed Ba onto Fe and Mn (oxyhydr)oxides (Carbonell et al., 1999).

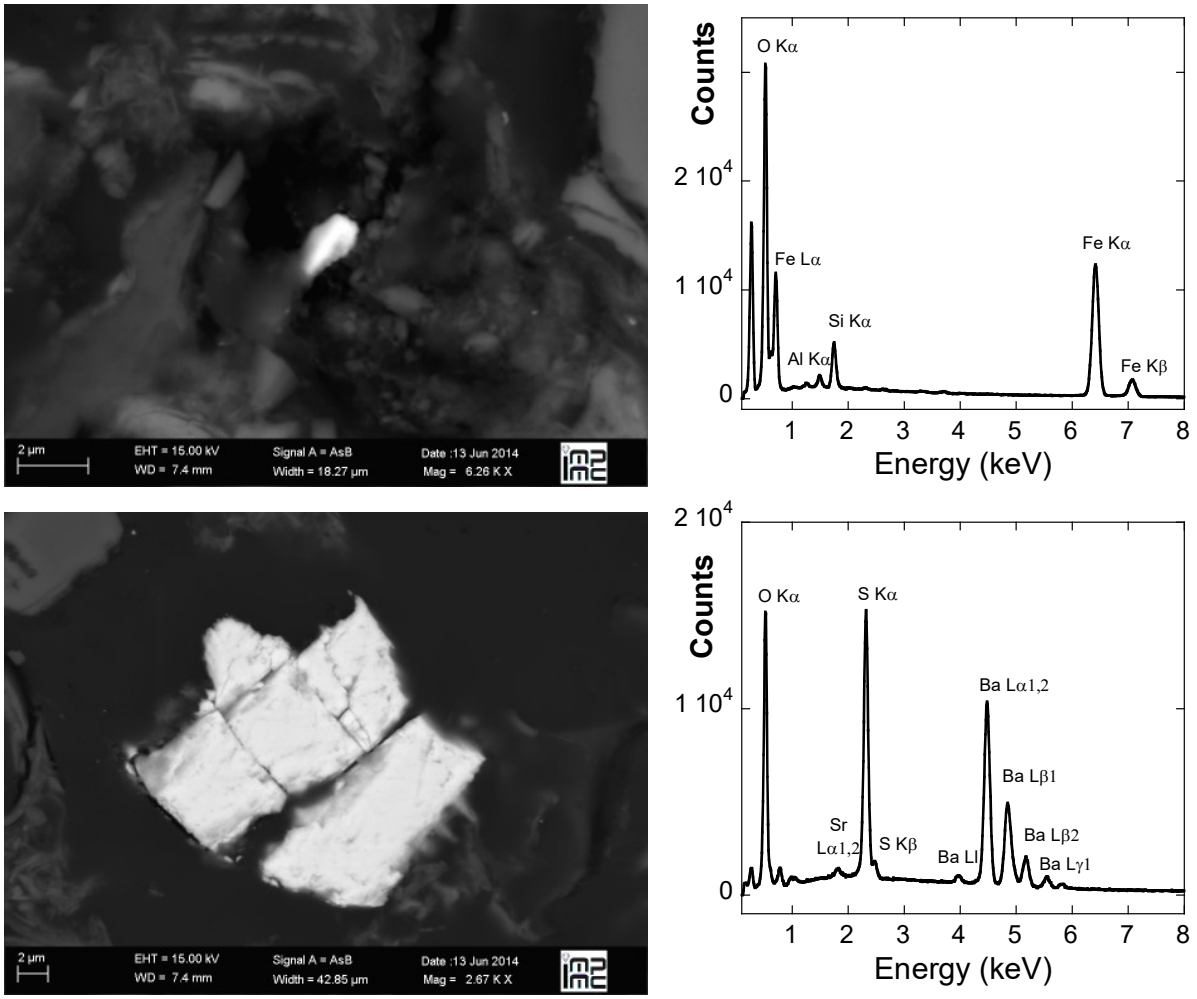


Fig. 6*: Backscattered SEM images and EDX spectra of an iron (oxyhydr)oxide grain in the 59 -62 cm depth sample (Top) and of barite crystals in the 143-146 cm depth sample (Bottom), from the sediment core collected in 2012 by Morin et al. (2016). Details on the SEM-EDXS analyses procedures are given in this previous study.*

Similarly, ^{226}Ra and ^{228}Ra activities seem to be correlated with Fe(II) in sediment pore waters, which suggests that the release of ^{226}Ra and ^{228}Ra from the SWI down to 40 cm depth may be related to the reductive dissolution of Fe and Mn (oxyhydr)oxides (Figure 3). The release of radium in the dissolved phase due to microbial Fe(III) reduction was previously identified using laboratory incubation experiments of uranium mill tailings under anaerobic conditions (Landa et al., 1991). However, the contribution of Mn-oxides dissolution to the release of radium cannot be excluded due to the high affinity of these minerals for Ra sorption (Goonnea et al., 2008).

Because dissolved ^{226}Ra and ^{228}Ra are correlated with dissolved Ba in the sediment pore waters in the first 40 cm under the SWI, we infer that this correlation is best explained by the common release of these elements via the reductive dissolution Fe and Mn (oxyhydr)oxides hosts phases. It is unlikely that the remobilization of radium in the sediments would be mainly controlled by sulfate reduction and subsequent dissolution of sulfate minerals such as strontianite, gypsum or barite. Indeed, SEM-EDXS observations of the sediments (Morin et al., 2016 ; Stetten et al. 2017) indicated the absence of gypsum and the presence of rare but massive barite crystals (Figure 6), and dissolved sulfide was found to be below detection limit of colorimetric methods in the study by Stetten et al. (2017).

Be 40 and 90 cm depth, the apparent correlation between dissolved Ba and Mn remains consistent with the reductive dissolution of Mn oxides, which are known to be excellent scavengers for Ba **(**Carbonell et al., 1998**)** This correlation, that is observed along the whole sediment column, suggests that the fraction potentially mobile Ba is dominantly hosted by Mn oxides. Besides, ^{226}Ra appears to be better correlated to dissolved Fe(II), which suggests that the reductive dissolution of Fe(III) (oxyhydr)oxides may be the dominant process involved in ^{226}Ra release. This observation may indicate that the potentially mobile fraction of ^{226}Ra is

mainly hosted by Fe(III) (oxyhydr)oxides, without excluding a fraction of ^{226}Ra associated to Mn oxides.

Below 90 cm, the increase of ^{226}Ra activity in pore waters is not related to Fe but possibly to the deposition of Ra-enriched particles, as demonstrated by the elevation of solid ^{226}Ra activity (Figure 2). **).** On the contrary, the Fe concentration in pore waters remain globally constant below this depth**.** The two peaks of Fe concentrations at 42.5 and 87.5 cm in the sediment, correlated with Mn, Zn and Cu (Figure 5), does therefore not induce significant changes in the geochemical behavior of Fe.

Altogether, our results suggest that the increase of radium activities in pore waters down to 40 cm depth below the SWI (Figure 3, Table 3) can be explained by the dissolution of Fe and Mn (oxyhydr)oxides. The release of Ra may however be limited because these phases contain relatively low Ra concentrations, as evidenced by selective chemical extractions (< 7% of total Ra) (Figure 4). Similar behaviour was previously shown in sediments affected by the discharge of ^{226}Ra associated with phosphate fertilizer plants where radium was also mostly associated with refractory phases (Aguado et al., 2004). In the following section, we estimate the radium flux that diffuses through the SWI in order to evaluate the extent of Ra release into the water column.

3.4 Diffusive radium fluxes determination through the sediment-water interface

The radium distribution in the pore waters was used to calculate the fluxes of radium that diffuses across the SWI. To do so, we used the Fick's First Law:

$$J_x = -D_S^i \, \varphi \frac{dC}{dz} \qquad \text{(Eq. 1)}$$

where J_z is the radium diffusive flux ; D^i_S the diffusion coefficient in the sediment calculated from the data reported previously (Yuan-Hui and Gregory, 1974) ; φ the porosity of 0.8 and dc/dz the concentration gradient accross the SWI.

Equation 1 neglects physical processes such as advection, wave-induced transport and gas ebullition in the system. As a first approximation, biodiffusion and bioirrigation processes are also ignored due to the absence of data regarding the abundance and the number of benthic animals in our studied site. A mean porosity value of 0.8 is used for the calculation of the diffusive fluxes. The diffusion coefficient D_w0 in free water was corrected for the effect of temperature according to the Stockes-Einstein relation, assuming an in situ temperature of 15°C (Table 6). The sediment diffusivity was calculated according to Berner (1980). Diffusive fluxes of ^{226}Ra and ^{228}Ra were finally determinated according to activities measured at 10 cm above and 7.5 cm below the SWI.

Tab. 6*: Description of parameters used for the calculation of radium diffusive fluxes (*Yan-Hui and Gregory, 1974; **Berner, 1980)*

Calculation of diffusivity of Ra^{2+} in free water (D_w)	
$(D_w^0.\eta^0/T)_{T1} = (D_w^0.\eta^0/T)_{T2}$ with $(Dw\text{-}_{25°C}{}^0/Dw\text{-}_T{}^0) = (\eta_T{}^0/\eta_{25°C}{}^0).(298/T) = 2.19$*	
T - temperature of lake waters (°C)	15
$D_w^{25°C}$ for Ra^{2+} ($cm^2.s^{-1}$)*	$8.89.10^{-6}$
$D_w^{15°C}$ for Ra^{2+} ($cm^2.s^{-1}$)	$8.73.10^{-6}$
Calculation of sediment diffusivity (D_s)	
$Ds = D_w .\varphi^2$ **	
φ	0.8
D_S for Ra^{2+} ($cm^2.s^{-1}$)	$5.59.10^{-6}$

The ^{226}Ra and ^{228}Ra diffusive fluxes at the SWI in the lake Saint-Clément are reported in Table 7 and compared with fluxes reported in the literature for other types of Ra-enriched sediments

((Martin et al., 2003; Gao et al., 2010; Handcock et al., 2010). In these latter studies fluxes calculations were made with 5-7 times higher resolution in the Ra pore water profiles than those in this study. However, our approach contributes to increase the knowledge on radium environmental geochemistry since i) to our knowledge, the data regarding Ra diffusive fluxes in fresh sediments impacted by former uranium mining activities are scarce and ii) this calculation is an useful step for the assessment of risks regarding the degree of radium mobilization.

Tab. 7: *Estimation of diffusive fluxes from the sediments of the lake Saint-Clément (mol.cm^{-2}.s^{-1}) compared with available data in the literature in other Ra-enriched sediments.*

	2016		Q1	Q5	W0	W2	W5
	This study	Handcock et al. (2000)	Martin et al. (2003)		Gao et al. (2010)		
	U-mining impacted lake sediments	Shallow lagoon	Uranium mill tailings pond		River sediment impacted by a phosphate plant		
Solid sediment activity (Bq.kg^{-1})	500	37-42	Not determined		< 180	84	2100
			Diffusive fluxes (mol.cm^{-2}.s^{-1})				
^{226}Ra	3.7.10^{-25}	3.5.10^{-25}	3.5.10^{-23}	1.2.10^{-20}	9.3.10^{-22}	1.9.10^{-21}	4.3.10^{-22}
^{228}Ra	1.1.10^{-27}	1.6.10^{-28}	-	-	-	-	-

The ^{226}Ra diffusive fluxes calculated here (3.7.10^{-25} mol.cm^{-2}.s^{-1}) are significantly lower than the values previously determined in the sediment of the Winterbeek river impacted by discharges from a phosphate plant in Belgium (Gao et al., 2010) and in an uranium mill tailings pond at Rio Algom's Quirke Mine in Canada (Martin et al., 2003). These two sites constitute two rare field cases where ^{226}Ra diffusive fluxes were determined in the context of former

industrial activities involving uranium extraction. We note that the diffusive fluxes of ^{226}Ra and ^{228}Ra reported here for lake Saint-Clément sediments are in the same order of magnitude as those determined from sediments of the Bega river estuary in Australia (Hancock et al., 2000). The differences discussed above in terms of diffusive ^{226}Ra fluxes cannot be attributed to the amount of ^{226}Ra in the sediments. Indeed, the Ra activity in sediments of the lake Saint-Clément is in the range of the Ra activity of the Winterbeek river sediments whereas the radium fluxes reported here are three to four orders of magnitude lower (Table 5). Secondly, for Rio Algom's Quirke Mine, the diffusive ^{226}Ra fluxes for this site were higher by two orders of magnitude than in the lake Saint-Clément, notably for the station Q1, in which dissolved oxygen concentrations in the bottom overlying waters were close to those encountered in the lake Saint-Clément. However, the ^{226}Ra activities in mill tailings are not reported (Martin et al., 2003) but could be possibly one to two orders of magnitude larger than in the sediments of the lake Saint-Clément (Abdelouas, 2006). Finally, the total solid ^{226}Ra in Bega estuarine sediments (50-105 Bq.kg^{-1}) are 5 to 10 times lower than in those of the lake Saint-Clément. It therefore confirms that the sedimentary Ra activity level alone does not explain the differences of ^{226}Ra fluxes for each site.

Overall, this short comparative analysis of various sites suggests that the combined effects of the sediment or tailing redox state and of the Ra solid speciation, notably the amount of Ra associated to redox-sensitive phases, can exert an important role in the ^{226}Ra diffusive flux. Indeed, the study of Martin et al. (2003) indicated that sub-oxic conditions exhibited minor ^{226}Ra fluxes while the development of anoxia contributed to a larger flux of ^{226}Ra. Secondly, th increased mobility of ^{226}Ra was found to be related to the dissolution of redox-sensitive ^{226}Ra solid phases such as barite.

4 Conclusions

This study reported original data regarding the effects of early diagenesis on the mobility of radium isotopes in the sediments of the lake Saint-Clément, located downstream from a former uranium mining site. Determination of the radium activities was successfully performed for the first time in small pore water volumes, carefully sampled under inert atmosphere, using well-type Germanium detectors, which is challenging.

Our results suggest that the Ra released in sediment pore water of the lake Saint-Clément is associated with the reductive dissolution of Fe and Mn (oxyhydr)oxides. This study demonstrates that even if Fe and Mn (oxyhydr)oxides and possibly natural organic matter are minor Ra-bearing phasesma,, the Ra released in sediment pore waters seems to be significantly driven by reductive dissolution of Fe and Mn (oxyhydr)oxides due to early diagenesis processes. The resulting diffusive Ra fluxes through the SWI remain low in the lake Saint-Clément. These fluxes are significantly lower than those previously reported in Ra-enriched sediments, suggesting that the Ra fluxes in lake Saint-Clément are not driven by the dissolution of Ra-bearing minerals such as e. g. barite ($BaSO_4$).

Further studies are needed for i) constraining the fate of natural organic matter and its association with radium isotopes when reducing conditions develop in the sediment and ii) improving the characterization of the other mechanisms (e. g. biodiffusion, bioturbation, gas bubbling and resuspension events) that may be involved in the early diagenesis of natural radionuclides..

Acknowledgements

We thank Anthony Julien, Olivier Diez and Marine Garcia for their help in field sampling and chemical analyses, respectively. This work was supported by the federator project Needs-

Environnement and IRSN (RASEDIM project). We are really grateful to Electricité De France (EDF) for the access of the lake Saint-Clément.

References

Abdelouas, A., 2006. Uranium mill tailings: geochemistry, mineralogy, and environmental impact. Elements 2, 335-341.

Aguado, J.L., Bolivar, J.P., Garcia-Tenorio, R., 2004. Sequential extraction of 226Ra in sediments from an estuary affected historically by anthropogenic inputs of natural radionuclides. J. Environ. Radioact. 74, 117-126.

Berner, R. A (1980) Early diagenesis. Princeton University Press.

Carbonell, A. A., De Laune, R. D., Patrick Jr, W. H., 1998. Effect of phosphogypsum and barite amendments on heavy metals and trace elements chemistry in Mississipi river alluvial sediment. J. Environ. Sci. Health Part A. 28, 316-321.

Carvalho, F.P., Oliveira, J.M., Malta, M., Lemos, M.E., 2014. Radioanalytical assessment of environmental contamination around non-remediated uranium mining legacy site and radium mobility. J. Radioanal. Nucl. Chem. 299, 119–125.

Cazala, C., Reyss, J.L., Decossas, J.L., Royer, A., 2003. Improvement in the Determination of 238U, 228-234Th, 226-228Ra, 210Pb, and 7Be by γ Spectrometry on Evaporated Fresh Water Samples. Environ. Sci. Technol. 37, 4990–4993. https://doi.org/10.1021/es034333i

Chen, M.A., Kocar, B.D., 2018. Radium Sorption to Iron (Hydr)oxides, Pyrite, and Montmorillonite: Implications for Mobility. Environ. Sci. Technol. 52, 4023–4030. https://doi.org/10.1021/acs.est.7b05443.

Doerner, H.A., Hoskins, W.M., 1925. Co-Precipitation of Radium and Barium Sulfates. J. Am. Chem. Soc. 47, 662–675.

Fadrus, H., Malý, J., 1975. Rapid extraction-photometric determination of traces of iron (II) and iron (III) in water with 1, 10-phenanthroline. Anal. Chim. Acta 77, 315–316.

Gao, Y., Baeyens, W., De Galan, S., Poffijn, A., Leermakers, M., 2010. Mobility of radium and trace metals in sediments of the Winterbeek: Application of sequential extraction and DGT techniques. Environ. Pollut. 158, 2439–2445. https://doi.org/10.1016/j.envpol.2010.03.022.

Goonnea, M.E., Morris, P.J., Dulaiova, H., Charrette, M.A. 2008. New perspectives on radium behaviour with a subterranean estuary. Mar. Chem. 109, 250-267.

Greeman, D. J., Rose, A. W., Washington, J. W., Dobos, R. R., Ciolkosz, E. J., 1999. Geochemistry of radium in soils of the Eastern United States. Geochimica et Cosmochima Acta. 14, 365-385.

Hancock, G.., Webster, I.., Ford, P.., Moore, W.., 2000. Using Ra isotopes to examine transport processes controlling benthic fluxes into a shallow estuarine lagoon. Geochim. Cosmochim. Acta 64, 3685–3699. https://doi.org/10.1016/S0016-7037(00)00469-5.

Henkel, S., Mogollón, J.M., Nöthen, K., Franke, C., Bogus, K., Robin, E., Bahr, A., Blumenberg, M., Pape, T., Seifert, R., März, C., de Lange, G.J., Kasten, S., 2012. Diagenetic barium cycling in Black Sea sediments – A case study for anoxic marine environments. Geochim. Cosmochim. Acta 88, 88–105. https://doi.org/10.1016/j.gca.2012.04.021.

International Atomic Energy Agency 2014. The environmental behaviour of radium: revised edition. Technical reports series no. 476.

Krest, J.M., Harvey, J.W., 2003. Using natural distributions of short-lived radium isotopes to quantify groundwater discharge and recharge. Limnol. Oceanogr. 48, 290–298. https://doi.org/10.4319/lo.2003.48.1.0290.

Landa, E. R., Gray, J. R. 1995. US Geological Survey-Research on the environmental fate of uranium mining and milling wastes. Env. Geol. 26, 19-31.

Landa, E.R., Phillips, E.J.P., Lovley, D.R., 1991. Release of226Ra from uranium mill tailings by microbial Fe(III) reduction. Appl. Geochem. 6, 647–652. https://doi.org/10.1016/0883-2927(91)90075-Z.

Martin, A.., Crusius, J., Jay McNee, J., Yanful, E.., 2003. The mobility of radium-226 and trace metals in pre-oxidized subaqueous uranium mill tailings. Appl. Geochem. 18, 1095–1110. https://doi.org/10.1016/S0883-2927(02)00243-3.

Mehra, O.P., Jackson, M.L., 2013. Iron oxide removal from soils and clays by a dithionite-citrate system buffered with sodium bicarbonate, in: Ingerson, E. (Ed.), Clays and Clay Minerals. Pergamon, pp. 317–327. https://doi.org/10.1016/B978-0-08-009235-5.50026-7.

Moore, R. W. S., 1996. Using the radium quartet for evaluating groundwater input and water exchange in salt marshes. Geochimica et Cosmochimica Acta. 60, 4645-4652.

Morin, G., Mangeret, A., Othmane, G., Stetten, L., Seder-Colomina, M., Brest, J., Ona-Nguema, G., Bassot, S., Courbet, C., Guillevic, J., 2016. Mononuclear U (IV) complexes and ningyoite as major uranium species in lake sediments. Geochem. Perspect. Lett. 2, 95–105.

Nirdosh, I., Muthuswami, S.V., Baird, M.H.I., 1984. Radium in uranium mill tailings - Some observations on retention and removal. Hydrometallurgy 12, 151–176. https://doi.org/10.1016/0304-386X(84)90032-X.

Nirdosh, I., Trembley, W.B., Johnson, C.R., 1990. Adsorption-desorption studies on the ^{226}Ra-hydrated metal oxide systems. Hydrometallurgy 24, 237–248.https://doi.org/10.1016/0304-386X(90)90089-K.

Peacey, V., Yanful, E. K., Payne, R. 2002. Field study of geochemistry and solute fluxes in flooded uranium mill tailings. Can. Geotech. J. 39, 357-376.

Reyss, J.-L., Mangeret, A., Courbet, C., Bassot, S., Alcalde, G., Thouvenot, A., Guillevic, J., 2016. Estimation of sedimentation rates based on the excess of radium 228 in granitic reservoir sediments. J. Environ. Radioact. 162–163, 8–13. https://doi.org/10.1016/j.jenvrad.2016.04.032.

Reyss, J.-L., Schmidt, S., Legeleux, F., Bonté, P., 1995. Large, low background well-type detectors for measurements of environmental radioactivity. Nucl. Instrum. Methods Phys. Res. Sect. Accel. Spectrometers Detect. Assoc. Equip. 357, 391–397. https://doi.org/10.1016/0168-9002(95)00021-6.

Rihs, S., Prunier, J., Thien, B., Lemarchand, D., Pierret, M.-C., Chabaux, F., 2011. Used short-lived nuclides of the U- and Th-series to probe the kinetics of colloid migration in forested soils. Geochimica et Cosmochimica Acta. 75,7706-7724.

Sebesta, F., Sedlacek, J., John, J., Sandrik, R., 1981. Behavior of radium and barium in a system including uranium mine waste waters and adjacent surface waters. Environ. Sci. Technol. 15, 71-75.

Stetten, L., Mangeret, A., Brest, J., Seder-Colomina, M., Le Pape, P., Ikogou, M., Zeyen, N., Thouvenot, A., Julien, A., Alcalde, G., Reyss, J.L., Bombled, B., Rabouille, C., Olivi, L., Proux, O., Cazala, C., Morin, G., 2018a. Geochemical control on the reduction of U(VI) to mononuclear U(IV) species in lacustrine sediments. Geochim. Cosmochim. Acta 222, 171–186. https://doi.org/10.1016/j.gca.2017.10.026.

Stetten, L., Blanchart, P., Mangeret, A., Lefebvre, P., Le Pape, P., Brest, J., Merrot, P., Julien, A., Proux, O., Webb, S.M., Bargar, J.R., Cazala, C., Morin., G., 2018b. Redox fluctuations and organic complexation govern uranium redistribution from U(IV)-

phosphate minerals in a mining-polluted wetland soil, Brittany, France. Environ. Sci. Tech. 52, 13099-13109.

Sun, Y., Torgersen, T., 2001. Adsorption–desorption reactions and bioturbation transport of ^{224}Ra in marine sediments: a one-dimensional model with applications. Mar. Chem. 74, 227–243. https://doi.org/10.1016/S0304-4203(01)00017-2.

Wiles, 1983. The radiochemistry of radium and thorium in uranium-mine tailings. Wat. Air & Soil Pol. 20, 99-108.

Yuan-Hui, L., Gregory, S., 1974. Diffusion of ions in sea water and in deep-sea sediments. Geochim. Cosmochim. Acta 38, 703–714.